Alkali Metal Complexes of the Pendant Arm Macrocyclic Ligand 1,4,7,10-Tetrakis(2-methoxyethyl)-1,4,7,10-tetraazacyclododecane. An Equilibrium and Inter- and Intramolecular Exchange Study

Ashley K. W. Stephens, Ramesh S. Dhillon, Samer E. Madbak, Sonya L. Whitbread, and Stephen F. Lincoln*

Department of Chemistry, University of Adelaide, Adelaide, SA 5005, Australia

Received August 2, 1995[⊗]

The stability constant, *K*, of the alkali metal complexes of 1,4,7,10-tetrakis(2-methoxyethyl)-1,4,7,10-tetraazacyclododecane, $[M(tmec12)]^+$, varies as M^+ changes in the sequence Li^+ (9.34 ± 0.05, 4.1 ± 0.1, and 3.61 ± 0.05), Na^+ (9.13 ± 0.05, 6.2 ± 0.1, and 5.68 ± 0.05), K^+ (6.07 ± 0.05, 3.9 ± 0.1, and 3.62 ± 0.05), Rb^+ (4.85 ± 0.05, 3.0 ± 0.1, and 2.73 ± 0.05), Cs^+ (3.55 ± 0.05, 2.5 ± 0.1, and 2.28 ± 0.05), and Ag^+ (12.30 ± 0.05, 14.2 ± 0.1, and 13.73 ± 0.05), where the figures in parentheses are $\log(K/dm^3\ mol^{-1})$ in acetonitrile, methanol, and dimethylformamide, respectively, determined by potentiometric titration at 298.2 K and $I = 0.05$ mol dm^{-3} (NEt_4ClO_4). Analogous data are obtained in propylene carbonate and dimethyl sulfoxide. For monomolecular $[Li(tmec12)]^+$ and $[Na(tmec12)]^+$ decomplexation in dimethylformamide k_d(298.2 K) = 31.4 ± 0.4 and 7.6 ± 0.3 s^{-1}, $\Delta H_d^{\ddagger}$ = 54.3 ± 0.5 and 76.2 ± 0.1 kJ mol^{-1}, and $\Delta S_d^{\ddagger}$ = −34.3 ± 1.5 and 27.7 ± 1.7 J K^{-1} mol^{-1}, respectively, determined by ^7Li and ^{23}Na NMR spectroscopy, and analogous data are reported for methanol and dimethyl sulfoxide solutions. The enantiomerization of Δ and Λ square antiprismatic $[Li(tmec12)]^+$ and their Na^+ and K^+ analogues in methanol, for which k_e(298.2 K) = 32800 ± 2400, 1470 ± 100, and 415 ± 4 s^{-1}, $\Delta H_e^{\ddagger}$ = 41.4 ± 0.5, 31.4 ± 0.9, and 50.7 ± 0.2 kJ mol^{-1} and $\Delta S_e^{\ddagger}$ = −19.7 ± 2.6, −78.8 ± 3.5, and −24.7 ± 0.7 J K^{-1} mol^{-1}, respectively, occurs much more rapidly than intermolecular tmec12 exchange on these complexes.

Introduction

The complexation of alkali metal ions by multidentate ligands involves sequential solvent displacement at the metal center and ligand conformational changes and sometimes results in the selective complexation of a particular alkali metal ion as exemplified by antibiotic complexes, coronates, and cryptates.[1−6] However, it is rarely the case that such complexation produces chiral complexes from an achiral ligand and that solution studies simultaneously yield information on stereochemistry and inter- and intramolecular exchange processes to the extent which we now report for the alkali metal complexes of 1,4,7,10-tetrakis-(2-methoxyethyl)-1,4,7,10-tetraazacyclododecane.[7,8] It is found that the square antiprismatic Δ and Λ enantiomers of $[M(tmec12)]^+$, M^+ and tmec12 exist in the equilibria shown in Figure 1, in which k_c, k_d, and k_e are the complexation, decomplexation and enantiomerization rate constants, respectively, and that the magnitude of the stability constant for $[M(tmec12)]^+$ ($K = k_c/k_d$) and its variation with the nature of M^+ is dependent on the nature of the solvent. These observations provide insight into the inter- and intramolecular complexation processes of $[M(tmec12)]^+$ and afford comparisons with other alkali metal complexes.

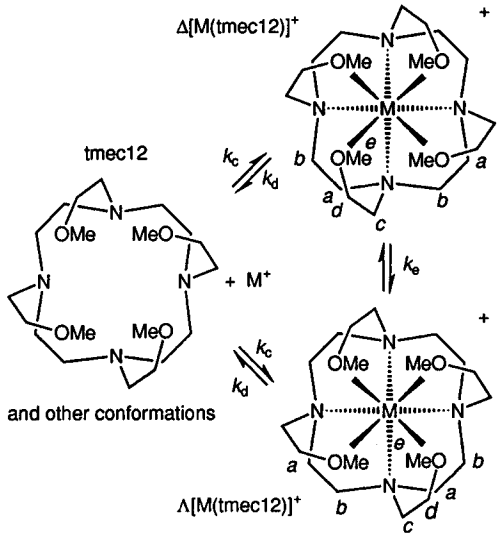

Figure 1. Scheme showing M^+ exchange and enantiomerization of $[M(tmec12)]^+$.

Experimental Section

The preparations of tmec12 and the sources of the alkali metal and silver perchlorates were similar to those described in the literature.[7] NEt_4ClO_4 was prepared by precipitation from aqueous NEt_4Br (BDH) solution with excess $HClO_4$ and was recrystallized from water until no acid or bromide was detectable. KCF_3SO_3 was prepared by reacting the stoichiometric amounts of K_2CO_3 (BDH) and CF_3SO_3H (Fluka) in water and twice recrystallizing the product from water. All the salts were vacuum dried at 353−363 K for 48 h and were then stored over P_2O_5 under vacuum. (***Caution***! Anhydrous perchlorate salts are potentially powerful oxidants and should be handled with care.)

Acetonitrile, methanol, propylene carbonate, dimethyformamide and dimethyl sulfoxide were purified and dried by literature methods.[9] Acetonitrile and methanol were stored over Linde 3 Å molecular sieves

[⊗] Abstract published in *Advance ACS Abstracts,* February 1, 1996.

(1) Lindoy, L. F. *The Chemistry of Macrocyclic Ligand Complexes*, Cambridge University Press: Cambridge, England, 1989.
(2) Izatt, R. M.; Pawlak K.; Bradshaw, J. S.; Bruening, R. L. *Chem. Rev.* **1991**, *91*, 1721−2085.
(3) Gokel, G. W. *Chem. Soc. Rev.* **1992**, 39−47.
(4) Gokel, G. W. *Crown Ethers and Cryptands*; The Royal Society of Chemistry: Cambridge, England, 1991.
(5) Lehn, J.-M.; Sauvage, J. P. *J. Am. Chem. Soc.* **1975**, *97*, 6700−6707.
(6) Lehn, J.-M. *Acc. Chem. Res.* **1978**, *11*, 49−57.
(7) Stephens, A. K. W.; Lincoln, S. F. *J. Chem. Soc., Dalton Trans.* **1993**, 2123−2126. (The ^{13}C chemical shifts for $-CH_2O-$ and $-OCH_3$ were inadvertently transposed in this reference.)
(8) Dhillon, R.; Stephens, A. K. W.; Whitbread, S. L.; Lincoln, S. F.; Wainwright, K. P. *J. Chem. Soc., Chem. Commun*, **1995**, 97−98.

0020-1669/96/1335-2019$12.00/0

Table 1. Stability Constants for $[M(tmec12)]^+$ and $[M(thec12)]^+$ at 298.2 K and $I = 0.05$ mol dm^{-3} (NEt_4ClO_4)

			log(K/dm^3 mol^{-1})					
complex	solvent	D_N	$M^+ = Li^+$	$M^+ = Na^+$	$M^+ = K^+$	$M^+ = Rb^+$	$M^+ = Cs^+$	$M^+ = Ag^+$
$[M(tmec12)]^+$ [a]	acetonitrile	14.1[b]	9.34 ± 0.05	9.13 ± 0.05	6.07 ± 0.05	4.85 ± 0.05	3.55 ± 0.05	12.30 ± 0.05
$[M(tmec12)]^+$ [a]	propylene carbonate	15.1[b]	8.0 ± 0.1	8.2 ± 0.1	6.7 ± 0.1	6.2 ± 0.1	low sol	15.3 ± 0.1
$[M(tmec12)]^+$ [a]	methanol	19.0[b]	4.1 ± 0.1	6.2 ± 0.1	3.9 ± 0.1	3.0 ± 0.1	2.5 ± 0.1	14.2 ± 0.1
		23.5[c]						
$[M(tmec12)]^+$ [a]	dimethylformamide	26[b]	3.61 ± 0.05	5.68 ± 0.05	3.62 ± 0.05	2.73 ± 0.05	2.28 ± 0.05	13.73 ± 0.05
$[M(tmec12)]^+$ [a]	dimethyl sulfoxide	29.8[b]	2.82 ± 0.05	4.95 ± 0.05				11.48 ± 0.05
$[M(tmec12)]^+$ [d]	water	18.0[b]	<2	2.20	<2	<2	<2	12.62
		33.0[c]						
$[M(thec12)]^+$ [e]	methanol	19.0[b]	3.09	4.53	2.43	2.20	1.90	12.57
		23.5[c]						
$[M(thec12)]^+$ [e]	dimethylformamide	26.6[b]	2.99	3.37	1.59	1.39	1.23	11.16

[a] This work. Errors represent one standard deviation. [b] Reference 13. D_N determined in 1,2-dichloroethane. [c] Reference 14. D_N determined in bulk solvent which permits the establishment of intermolecular hydrogen bonding and may account for the higher D_N values by comparison with those from reference 13. [d] Reference 7. $I = 0.05$ mol dm^{-3} (NEt_4ClO_4). [e] Reference 11.

and the other three solvents over 4 Å molecular sieves under nitrogen. The water content of these solvents was below the Karl-Fischer detection level of ~50 ppm. Methanol-^{12}C-d_4 (99.95 atom % ^{12}C and 99.5% ^2H, Aldrich) was used as received. Solutions of anhydrous metal perchlorates (or KCF_3SO_3 for ^{13}C NMR studies as $KClO_4$ was insufficiently soluble to give reasonable resonance intensities) and tmec12 were prepared under dry nitrogen in a glovebox. For ^{13}C NMR studies, methanol-^{12}C-d_4 solutions of the appropriate alkali metal salt and tmec12 were transferred to tightly stoppered 5-mm NMR tubes. For ^7Li and ^{23}Na NMR studies, solutions were degassed and sealed under vacuum in 5-mm NMR tubes that were coaxially mounted in 10-mm NMR tubes containing either D_2O or acetone-d_6 that provided the deuterium lock signal. The stabilities of $[M(tmec12)]^+$ were sufficiently high for $[M(tmec12)]^+$ and free M^+ and tmec12 concentrations in the solutions prepared for the NMR studies to be those arising from the simple stoichiometric complexation of M^+ by tmec12.

^7Li, ^{13}C (broad-band ^1H decoupled) and ^{23}Na NMR spectra were run at 116.59, 75.47, and 79.39 MHz, respectively, on a Bruker CXP-300 spectrometer. In the ^7Li experiments 1000−6000 transients were accumulated in a 8192 data point base over a 1000 Hz spectral width. In the ^{13}C experiments 6000 transients were accumulated in a 8192 data point base over a 3000 Hz spectral width, and in the ^{23}Na experiments 1000−6000 transients were accumulated in a 2048 data point base over a 8000 Hz spectral width for each solution prior to Fourier transformation. Solution temperature was controlled to within ±0.3 K using a Bruker B-VT 1000 temperature controller. The Fourier transformed spectra were subjected to complete line shape analysis[10] on a VAX 11-780 computer to obtain kinetic data. The temperature dependent ^7Li, ^{13}C and ^{23}Na line widths and chemical shifts employed in the complete line shape analysis were obtained by extrapolation from low temperatures where no exchange induced modification occurred. Stability constants, K, were determined by triplicated potentiometric titrations using methods similar to those described in the literature.[11,12]

Results and Discussion

$[M(tmec12)]^+$ Stability. The stability constant, $K = [M(tmec12)^+]/([M^+][tmec12])$, varies with M^+ in the sequence $Li^+ \geq Na^+ > K^+ > Rb^+ > Cs^+$, in acetonitrile, $Li^+ \approx Na^+ > K^+ > Rb^+$ in propylene carbonate, and $Li^+ < Na^+ > K^+ > Rb^+ > Cs^+$ in methanol and dimethylformamide (Table 1). These variations in the sequence of $[M(tmec12)]^+$ stability, and the decrease in K, accompanying the increase in solvent electron donating power, as reflected by the Gutmann donor number (D_N),[13,14] are consistent with three factors dominating the stability of $[M(tmec12)]^+$: (i) the solvation energy of M^+, (ii) the electron donating power of the donor atoms of tmec12, and (iii) the ability of tmec12 to assume a conformation that optimizes bonding with M^+. Thus, as M^+ becomes more strongly solvated with increasing solvent electron donating power (D_N), there is a general decrease in K and the complex stability sequence changes as the balance among points i−iii changes.

In methanol, all four pendant arms are coordinated in $[Li(tmec12)]^+$, $[Na(tmec12)]^+$, and $[K(tmec12)]^+$ (see below), and it is assumed that a similar situation prevails with $[Rb(tmec12)]^+$ and $[Cs(tmec12)]^+$, which were not amenable to ^{13}C NMR studies due to the low solubilities of their salts. As acetonitrile and propylene carbonate compete less effectively with tmec12 for M^+ than does methanol, it is probable that $[M(tmec12)]^+$ is similarly coordinated in these solvents also and that coordination changes do not contribute to the variations in stability. The stability of $[M(tmec12)]^+$ is generally greater than that of $[M(thec12)]^+$ (where thec12 is 1,4,7,10-tetrakis(2-hydroxyethyl)-1,4,7,10-tetraazacyclododecane, an analogue of tmec12 in which all of the methoxy groups are replaced by hydroxy groups) in methanol and dimethylformamide (Table 1). This may be because either the methyl inductive effect causes the tmec12 methoxy groups to be stronger electron pair donors than are the thec12 hydroxy groups, or intramolecular hydrogen bonding in thec12 and hydrogen bonding with solvent compete with coordination to M^+, or a combination of these effects takes place.

The variation of the sequence of the relative magnitudes of K for $[M(tmec12)]^+$ with solvent contrasts with the constancy of the sequence of K variation with M^+ for the cryptate formed by 4,7,13,18,-tetraaoxa-1,10-diazabicyclo[8.5.5]icosane, $[M(C211)]^+$, which is $Li^+ > Na^+ > K^+ > Rb^+ > Cs^+$ and that for the cryptate formed by 4,7,13,16,21-pentaoxa-1,10-diazabicyclo[8.8.5]tricosane, $[M(C221)]^+$, which is $Li^+ < Na^+ > K^+ > Rb^+ > Cs^+$ in the solvents considered here and other solvents.[12,15] This is consistent with the relatively rigid cavity radii of C211 (80 pm) and C221 (110 pm)[4] more closely approximating the radii of six-coordinate Li^+ (76 pm) and seven-coordinate Na^+ (112 pm)[16] than those of the other M^+ and thereby conferring the highest stabilities on $[Li(C211)]^+$ and $[Na(C221)]^+$ while the flexibility of tmec12 results in lower

(9) Perrin, D. D.; Aramaego, W. L. F.; Perrin, D. R. *Purification of Laboratory Chemicals*, 2nd. ed.; Pergamon: Oxford, England, 1980.
(10) Lincoln, S. F. *Prog. React. Kinet.* **1977**, *9*, 1−91.
(11) Turonek, M. L.; Clarke, P.; Laurence, G. S.; Lincoln, S. F.; Pittet, P.-A.; Politis, S.; Wainwright, K. P. *Inorg. Chem.* **1993**, *32*, 2195−2198.
(12) Cox, B. G.; Schneider, H: Stroka, J. J. *J. Am. Chem. Soc.* **1978**, *100*, 4746−4749.
(13) Gutmann, V. *Coordination Chemistry in Nonaqueous Solutions*; Springer-Verlag: Vienna, 1968.
(14) Dewitte, W. J.; Popov, A. I. *J. Solution Chem.* **1976**, *5*, 231−240.
(15) Cox, B. G.; Garcia-Rosas, J.; Schneider, H. *J. Am. Chem. Soc.* **1981**, *103*, 1384-1389.
(16) Shannon, R. D. *Acta Crystallogr., Sect. A: Cryst. Phys. Diffr., Theor. Gen. Crystallogr.* **1976**, *A32*, 751−767.

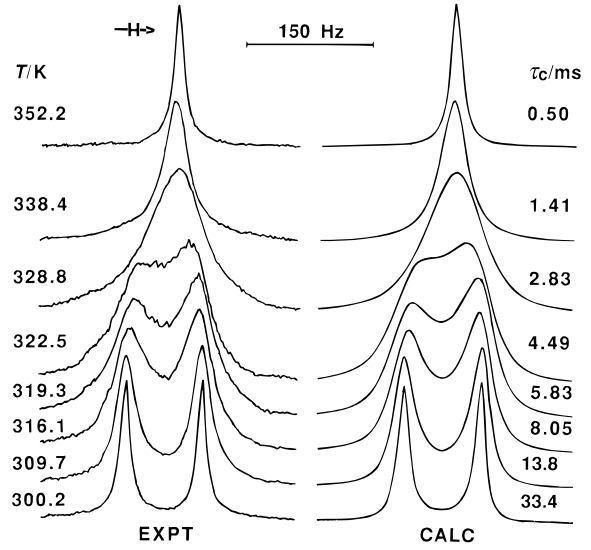

Figure 2. Typical exchange-modified 116.59 MHz ^{7}Li NMR spectra of a dimethyl sulfoxide solution of solvated Li^+ (0.0474 mol dm^{-3}) and $[Li(tmec12)]^+$ (0.0534 mol dm^{-3}). Experimental temperatures and spectra appear to the left of the Figure, and the best fit calculated line shapes and corresponding τ_c values appear to the right. The resonance of $[Li(tmec12)]^+$ appears downfield from that of solvated Li^+.

selectivities and stabilities for $[M(tmec12)]^+$. The much higher stabilities of $[Ag(tmec12)]^+$ and $[Ag(thec12)]^+$ by comparison with those of their alkali metal analogues arise from the strong affinity of soft acid[17,18] Ag^+ for nitrogen donor atoms,[19,20] and their lower stabilities in nitrogen donor acetonitrile also arises from this source.

$[M(tmec12)]^+$ Intermolecular Metal Ion Exchange. Complete line shape analyses[10] of the temperature dependent coalescences of the ^{7}Li and ^{23}Na resonances arising from exchange of these nuclei between the solvated M^+ and $[M(tmec12)]^+$ environments in methanol, dimethylformamide and dimethyl sulfoxide (Figure 2) yield the mean lifetime of M^+ in $[M(tmec12)]^+$, $\tau_c = X_c\tau_s/X_s$, where τ_s is the mean lifetime of M^+ in the solvated state, and X_c and X_s are the corresponding mole fractions for the solutions whose compositions are given in the caption to Figure 3. The magnitudes and temperature variations of τ_c for $[Li(tmec12)]^+$ in each group of solutions of a given solvent are very similar, as is also the case for $[Na(tmec12)]^+$ (Figure 3). Thus, τ_c is independent of the concentration of solvated M^+ consistent with its nonparticipation in the rate determining step for M^+ exchange on $[M(tmec12)]^+$ and the operation of a monomolecular mechanism for the decomplexation of M^+ from $[M(tmec12)]^+$ as shown in eq 1. The parameters for the decomplexation of $[M(tmec12)]^+$ (Table 2) were derived through a simultaneous fit of the τ_c data from all the solutions in a given solvent to eq 2.

$$M^+ + \text{tmec12} \underset{k_d}{\overset{k_c}{\rightleftharpoons}} [M(tmec12)]^+ \qquad (1)$$

$$k_d = 1/\tau_c = (k_B T/h)\exp(-\Delta H_d^{\ddagger}/RT + \Delta S_d^{\ddagger}/R) \qquad (2)$$

In dimethylformamide and dimethyl sulfoxide k_d for $[Li(tmec12)]^+$ is larger than that for $[Na(tmec12)]^+$. The smaller $\Delta H_d^{\ddagger}$ and smaller or more negative $\Delta S_d^{\ddagger}$ for $[Li(tmec12)]^+$ (by comparison with those for $[Na(tmec12)]^+$) may arise from a greater involvement of solvent in the process characterized by k_d than is the case for $[Na(tmec12)]^+$. A similar comparison holds for the more labile $[Li(thec12)]^+$ and $[Na(thec12)]^+$ in methanol and dimethylformamide. The second-order rate constant, k_c, is the product of the stability constant for the encounter complex (where tmec12 resides in the second coordination sphere in contact with the first coordination sphere of solvated M^+) formed at a rate close to diffusion control and the first-order rate constant for the subsequent rate determining complexation step. The decrease in k_c with increase in solvent D_N probably reflects a combination of the effect of solvent change on encounter complex stability and its effect on the solvation energy of M^+. Although the contributions from these two sources cannot be separated from the present data, the variation of k_c is consistent with M^+ desolvation being a significant determinant of the magnitude of k_c. The increase in k_c on going from $[Li(tmec12)]^+$ to $[Na(tmec12)]^+$ may also reflect the lower solvation energy anticipated for solvated Na^+ by comparison with that of Li^+, but a contribution to this increase may also arise from the differing amounts of strain induced in tmec12 on coordination of these ions.

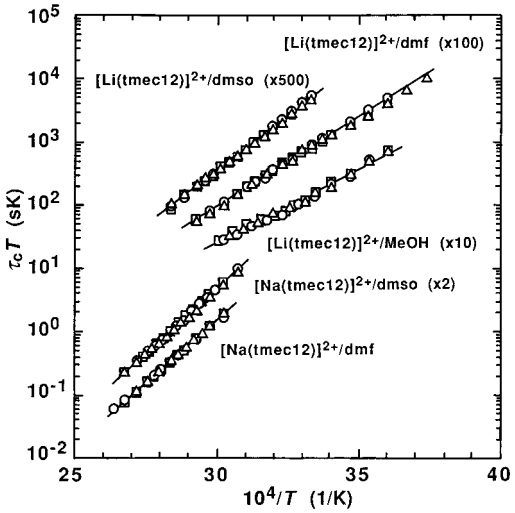

Figure 3. Temperature variations of τ_c for $[M(tmec12)]^+$. Data obtained from methanol (MeOH) solutions i−iii are represented by triangles, squares, and circles, and $[Li^+_{solvated}]$ and $[Li(tmec12)^+]$ are 0.00065 and 0.0141, 0.0090 and 0.0115, and 0.0128 and 0.0077 mol dm^{-3}, respectively. Data obtained from dimethylformamide (dmf) solutions iv−vi are represented by triangles, squares, and circles, and $[Li^+_{solvated}]$ and $[Li(tmec12)^+]$ are 0.0250 and 0.0749, 0.0454 and 0.0544, and 0.0639 and 0.0360 mol dm^{-3}, respectively. Data obtained from dimethyl sulfoxide (dmso) solutions vii−ix are represented by triangles, squares, and circles, and $[Li^+_{solvated}]$ and $[Li(tmec12)^+]$ are 0.0272 and 0.0736, 0.0474 and 0.0534, and 0.0600 and 0.0408 mol dm^{-3}, respectively. Data obtained from dimethyl sulfoxide solutions x−xii are represented by triangles, squares, and circles, and $[Na^+_{solvated}]$ and $[Na(tmec12)^+]$ are 0.0351 and 0.0653, 0.0502 and 0.0502, and 0.0673 and 0.0331 mol dm^{-3}, respectively. Data obtained from dimethylformamide solutions xiii−xvi are represented by triangles, squares, and circles, and $[Na^+_{solvated}]$ and $[Na(tmec12)^+]$ are 0.0259 and 0.0777, 0.0549 and 0.0487, and 0.0730 and 0.0306 mol dm^{-3}, respectively. The solid lines represent the best fits of the combined data for each group of solutions to eq 2.

At temperatures near the solution boiling point, Li^+ exchange on $[Li(tmec12)]^+$ in acetonitrile and propylene carbonate and Na^+ exchange on $[Na(tmec12)]^+$ in acetonitrile, propylene carbonate, and methanol were in the slow exchange limit of the NMR timescale, and the separate resonances of the metal nuclei in the solvated and complexed environments showed no significant broadening. Conservative lower limits were calculated corresponding to a τ_c that would cause a 0.5-fold broadening of the line width at half amplitude of the resonance

(17) Pearson, R. G. *J. Am. Chem. Soc.* **1963**, *85*, 3533−3539.
(18) Pearson, R. G. *Coord. Chem. Rev.* **1990**, *100*, 403−425.
(19) Cotton, F. A., Wilkinson, G. *Advanced Inorganic Chemistry*, 3rd. ed.; Interscience: New York, 1980.
(20) Buschmann, H.-J. *Inorg. Chim. Acta* **1985**, *102*, 95−98.

Table 2. Kinetic Parameters for Metal Ion Exchange on $[Li(tmec12)]^+$, $[Na(tmec12)]^+$, $[Li(thec12)]^+$, and $[Na(thec12)]^+$

complex	solvent	$10^{-5}k_c$(298.2 K), $dm^3\ mol^{-1}\ s^{-1}$	k_d(298.2 K), s^{-1}	$\Delta H_d^{\ddagger}$, kJ mol^{-1}	$\Delta S_d^{\ddagger}$, J $K^{-1}\ mol^{-1}$
$[Li(tmec12)]^{a}$	methanol	2.3	18.2 ± 0.4	44.8 ± 0.8	-70.5 ± 2.9
$[Li(tmec12)]^{+\,a}$	dimethyl formamide	1.3	31.4 ± 0.4	54.3 ± 0.5	-34.3 ± 1.5
$[Li(tmec12)]^{+\,a}$	dimethyl sulfoxide	0.17	25.6 ± 0.4	66.0 ± 0.5	3.3 ± 1.4
$[Na(tmec12)]^{+\,a}$	methanol		$\ll 50$		
$[Na(tmec12)]^{+\,a}$	dimethyl formamide	36.4	7.6 ± 0.3	76.2 ± 0.1	27.7 ± 1.7
$[Na(tmec12)]^{+\,a}$	dimethyl sulfoxide	4.1	4.6 ± 0.2	78.1 ± 0.1	29.6 ± 1.6
$[Na(tmec12)]^{+\,b}$	water	0.11	70	64.0	5.1
$[Li(thec12)]^{+\,c}$	methanol	8.97	729	38.0	−62.8
$[Li(thec12)]^{+\,c}$	dimethyl formamide	5.74	587	41.8	−51.9
$[Na(thec12)]^{+\,c}$	methanol	70.8	209	68.3	28.4
$[Na(thec12)]^{+\,c}$	dimethyl formamide	7.00	299	56.4	−8.4

[a] This work. Errors represent one standard deviation for the fit of eq 2 to the τ_c data. *b* Reference 7. *c* Reference 11.

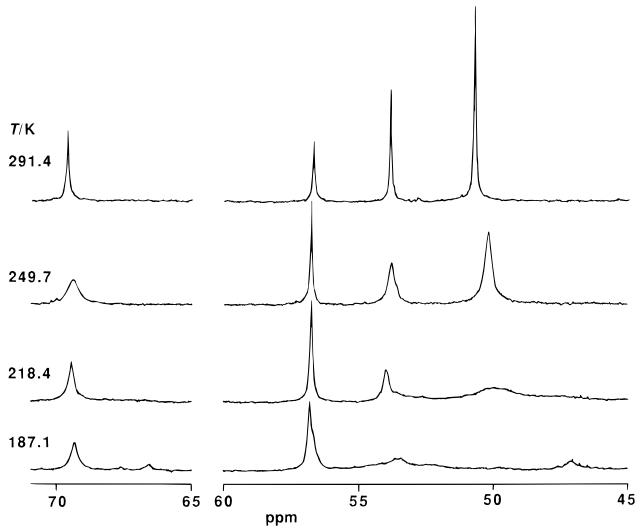

Figure 4. Temperature variation of the broad-band ^1H decoupled ^{13}C NMR spectrum (75.47 MHz) of a 0.10 mol dm^{-3} tmec12 solution in methanol-^{12}C-d_4. Experimental temperatures are indicated on the left-hand side of the figure.

arising from $[M(tmec12)]^+$, $W_{1/2c}$, such that $\tau_c = \pi W_{1/2c}/2$. On this basis upper limits of k_d <8.5 (355 K) and <11.9 s^{-1} (400 K) were obtained for $[Li(tmec12)]^+$ in acetonitrile and propylene carbonate, respectively, for $W_{1/2c} = 5.4$ and 7.6 Hz. For $[Na(tmec12)]^+$ upper limits of k_d < 41 (355 K), < 87 (400 K) and < 58 s^{-1} (338 K) were obtained in acetonitrile, propylene carbonate, and methanol, respectively, for $W_{1/2c} = 26.1$, 55.4, and 37.0 Hz.

$[M(tmec12)]^+$ Intramolecular Exchange. The broad-band ^1H decoupled ^{13}C NMR spectrum of tmec12 in methanol-^{12}C-d_4 exhibits a substantial temperature variation (Figure 4). At 270.5 K the pendant arm $-CH_2O-$, $-OCH_3$, $>NCH_2-$, and macrocyclic ring resonances are observed at 69.42, 56.77, 53.96, and 50.18 ppm, respectively.[7] As the temperature decreases the pendant arm $-CH_2O-$, $>NCH_2-$, and macrocyclic ring resonances broaden and partially resolve into several resonances at 187.1 K, while the $-OCH_3$ resonance appears close to resolution into two resonances at 187.1 K. In the tmec12 conformer shown in Figure 1, where the four oxygen atoms and four nitrogen atoms are at the corners of the opposed faces of a square antiprism, each pendant arm is equivalent so that singlet ^{13}C resonances should arise from each of the $-CH_2O-$, $-OCH_3$, $>NCH_2-$ carbons, whereas the macrocyclic ring carbons form two non-equivalent sets for which a singlet ^{13}C resonance should be seen in each case. While this may be one of the tmec12 conformers contributing to the ^{13}C spectral temperature dependence, it cannot be the sole conformer as observation of at least two resonances for each of the pendant arm carbons at 187.1 K is consistent with their inequivalence in other conformers. These data do not permit an indentification of the conformers present which contrasts with the $[M(tmec12)]^+$ data discussed below.

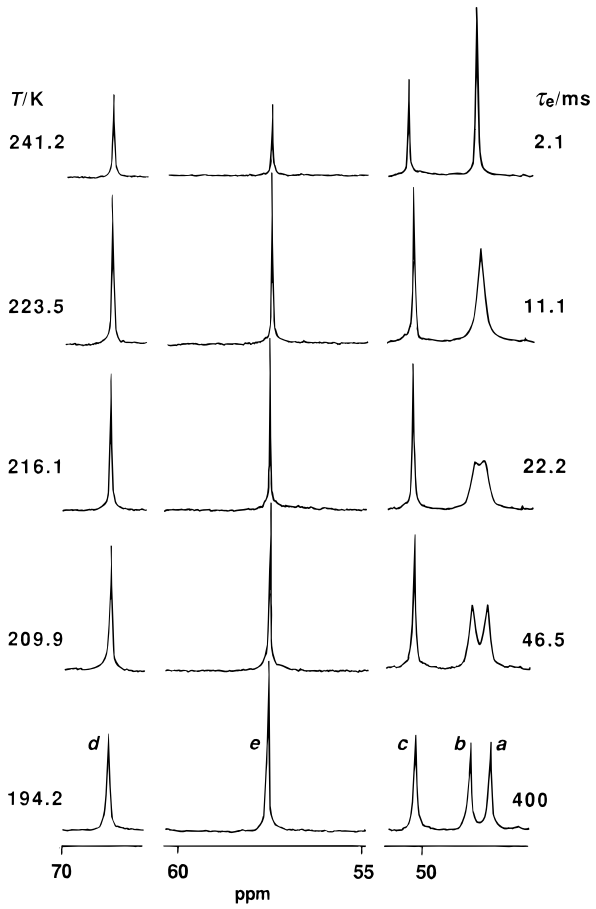

Figure 5. Temperature variation of the broad-band ^1H decoupled ^{13}C NMR spectrum (75.47 MHz) of a 0.10 mol dm^{-3} $[Li(tmec12)]^+$ solution in methanol-^{12}C-d_4. Experimental temperatures and τ_e values derived from complete line shape analyses of the coalescing doublet arising from the macrocylic ring carbons (*a* and *b*) appear on the left- and right-hand sides of the figure, respectively. The resonances arising from the pendant arm $-CH_2O-$ (*d*), $-OCH_3$ (*e*), and $>NCH_2-$ (*c*) carbons are indicated by italic letters.

Under slow exchange conditions at 209.9 K in methanol-^{12}C-d_4 , the broad-band ^1H decoupled ^{13}C NMR spectrum of $[Li(tmec12)]^+$ (Figure 5) consists of five resonances at 68.51, 57.37 and 50.05 ppm assigned to the pendant arm $-CH_2O-$, $-OCH_3$, and $>NCH_2-$ carbons, respectively, and at 48.50 and 48.05 ppm assigned to the macrocyclic ring carbons that cannot be separately identified from these data. Five similarly assigned resonances at 68.06, 57.48, 51.12, 48.68, and 47.79 ppm are

Table 3. Parameters for Enantiomerization and Ligand Exchange on $[M(tmec12)]^+$ and $[M(thec12)]+$ in Methanol-^{12}C-d_4

complex	process	k,[a] s^{-1}	k(298.2 K), s^{-1}	$\Delta H^{\ddagger}$, kJ mol^{-1}	$\Delta S^{\ddagger}$, J K^{-1} mol^{-1}
$[Li(tmec12)]^+$	enantiomerization	42 ± 1 (216.2 K)	32800 ± 2400	41.4 ± 0.5	−19.7 ± 2.6
	ligand exchange[b]	64.8 ± 1.4 (314.8 K)	23.0 ± 0.5	46.1 ± 0.6	−64 ± 2
$[Na(tmec12)]^+$	enantiomerization	84.3 ± 2.7 (246.4 K)	1470 ± 100	31.4 ± 0.9	−78.8 ± 3.5
	ligand exchange[c]		<14		
$[K(tmec12)]^+$	enantiomerization	21.8 ± 0.1 (262.1 K)	415 ± 4	50.7 ± 0.2	−24.7 ± 0.7
	ligand exchange[d]	196 ± 6 (314.8 K)	34.1 ± 1.6	79.9 ± 1.7	52.5 ± 5.8
$[Na(thec12)]^+$[e]	enantiomerization	1237 ± 17 (256.9 K)	7100 ± 216	24.6 ± 0.5	−88 ± 2
	ligand exchange	62 ± 2 (281.0 K)	332 ± 8	65.6 ± 0.8	23.3 ± 3.0

[a] Rate constant at coalescence temperature shown in parentheses. [b] Derived from the coalescence of the $-CH_2O-$ resonances of $[Li(tmec12)]^+$ and tmec12. [c] Too slow to determine. [d] Derived from the coalescence of the $-CH_2O-$ resonances of $[K(tmec12)]^+$ and tmec12. [e] Reference 8. Errors represent one standard deviation for the fit of eq 2 to either τ_e or τ_c data.

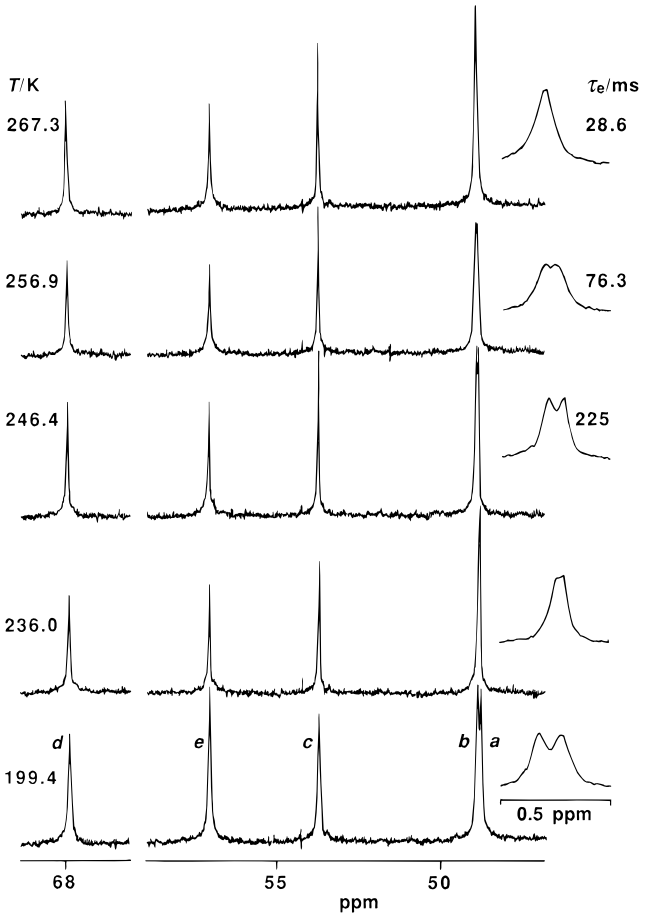

Figure 6. Variation with temperature of the broad-band ^1H decoupled 75.47 MHz ^{13}C NMR spectrum of a 0.10 mol dm^{-3} $[K(tmec12)]^+$ solution in methanol-^{12}C-d_4. Experimental temperatures and τ_e values derived from complete line shape analyses of the coalescing doublet arising from the macrocylic ring carbons (*a* and *b*), appear on the left- and right-hand sides of the figure, respectively. The *a* and *b* resonances are shown at an expanded frequency in the insets on the right-hand side of the figure. The spectra observed at 236.0 and 199.4 K show no significant exchange induced line shape modification, and together with that observed at 246.4 K, illustrate the temperature variation of $\Delta\delta$ of the macrocylic ring carbons. At 199.4 K the resonances arising from the pendant arm $-CH_2O-$ (*d*), $-OCH_3$ (*e*) and $>NCH_2-$ (*c*) carbons are indicated by italic letters.

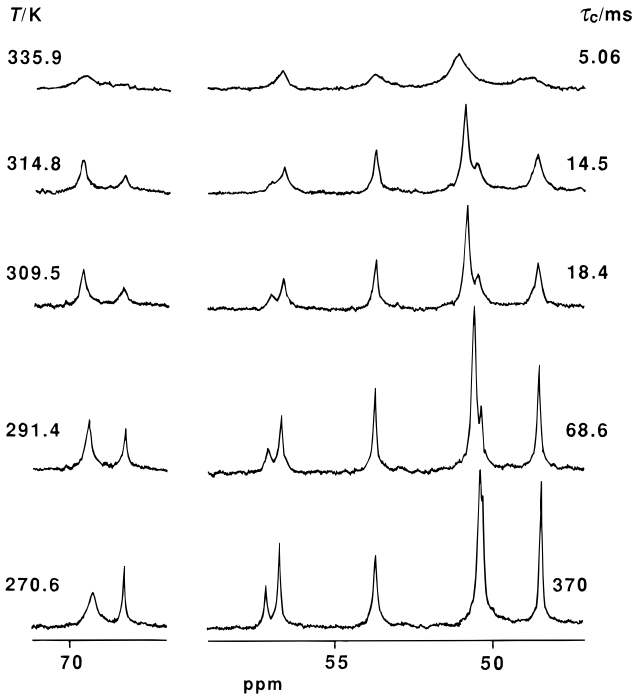

Figure 7. Temperature variation of the broad-band ^1H decoupled 75.47 MHz ^{13}C NMR spectrum of a 0.14 mol dm^{-3} and 0.05 mol dm^{-3} solution of tmec12 and $[Li(tmec12)]CF_3SO_3$, respectively, in methanol-^{12}C-d_4. Experimental temperatures and derived τ_c values appear on the left- and right-hand sides of the figure, respectively. At 291.4 K the resonances, from left to right of the spectrum, are assigned to tmec12 $-CH_2O-$, $[Li(tmec12)]^+$ $-CH_2O-$, $[Li(tmec12)]^+$ $-OCH_3$, tmec12 $-OCH_3$, tmec12 $>NCH_2-$, the macrocylic ring carbons of tmec12, $[Li(tmec12)]^+$ $>NCH_2-$, and the macrocylic ring carbons of $[Li(tmec12)]^+$.

observed for $[Na(tmec12)]^+$ [8] and for $[K(tmec12)]^+$ (Figure 6) at 68.00, 57.15, 53.80, 49.03, and 48.92 ppm. For $[Li(tmec12)]^+$, $[Na(tmec12)]^+$, and $[K(tmec12)]^+$, respectively, the difference in magnetic environments for $-CH_2O-$ and $>NCH_2-$ are reflected in $\Delta\delta$ decreases in the sequence 18.46, 16.94, and 14.20 ppm whereas it varies for the macrocylic ring carbons in the sequence 0.45, 0.89, and 0.11 ppm.

The two $[Li(tmec12)]^+$ resonances at higher field broaden and coalesce as the two macrocylic ring carbons exchange between different magnetic environments. Similar coalescences are observed for $[Na(tmec12)]^+$ [8] and $[K(tmec12)]^+$ with that of the latter being complicated by the temperature dependent shifts of the macrocylic ring resonances resulting in a reversal of their relative chemical shifts below the temperature at which exchange induced modification occurs (Figure 6). Complete line shape analyses of these coalescences yield the rate parameters in Table 3. For $[Li(tmec12)]^+$, these parameters were derived from the following mean enantiomer lifetime, τ_e, (ms) values determined in the temperature range where the exchange-induced resonance modifications were substantial and where the values in parentheses are the corresponding temperatures (K): 400 (194.3), 100 (204.8), 46.5 (210.0), 29.0 (213.1), 22.2 (216.2), 17.2 (220.4), 11.1 (223.6), 6.80 (226.7), 5.20 (230.9), 2.07 (241.3), 0.79 (251.7), and 0.34 (261.2). The corresponding data for $[Na(tmec12)]^+$ are 3.08 (230.8), 2.54 (236.0), 1.73 (241.2), 1.45 (246.4), 1.05 (251.6), 0.84 (256.9), 0.65 (262.1), 0.38 (272.5), 0.30 (277.8), and 0.26 (283.0), and the data for $[K(tmec12)]^+$ are 225 (246.4), 128 (251.6), 76.3

(256.9), 45.5 (262.1), 28.6 (267.3), 17.5 (272.5), 11.8 (277.7), 7.69 (283.0), and 3.33 (293.8).

The coalescence of the two macrocyclic ring resonances of $[Li(tmec12)]^+$ and those of the Na^+ and K^+ analogues, and the absence of change in their pendant arm resonances, apart from a slight broadening attributable to solution viscosity increases at lower temperatures, is consistent with exchange between two square antiprismatic $[M(tmec12)]^+$ enantiomers (Figure 1). Enantiomerization interchanges the magnetic environments of the macrocyclic ring carbons at sites *a* and *b*, whereas the pendant arm carbons in sites *c*−*e* experience no change in magnetic environment. The square antiprismatic $[M(tmec12)]^+$ enantiomer structures are probably similar to that seen in the solid state for $[K(thec12)]^+$.[21] The enantiomerization of $[Li(tmec12)]^+$ and $[Na(tmec12)]^+$ occurs much more rapidly than the intermolecular exchange of Li^+ and Na^+ between the solvated and complexed environments in methanol as is seen from Tables 2 and 3.

$[M(tmec12)]^+$ Intermolecular Ligand Exchange. Intermolecular exchange between free tmec12 and either $[Li(tmec12)]^+$ or $[K(tmec12)]^+$ (eq 3) is indicated by the coalescence of the $-CH_2O-$, $-OCH_3$, and $>NCH_2-$ ^{13}C resonances of the free and complexed tmec12 (Figure 7) and is characterized by the parameters in Table 3. For $[Li(tmec12)]^+$, these parameters were derived from the complete line shape analysis of the coalescence of the $-CH_2O-$ resonances which exhibited the largest $\Delta\delta$, and which yielded the following mean $[Li(tmec12)]^+$ lifetimes, τ_c (ms), where the values in parentheses are the corresponding temperatures (K): 1610 (249.7), 1180 (254.9), 770 (260.1), 565 (265.3), 370 (270.6), 218 (275.8), 142 (281.0), 105 (286.2), 68.5 (291.4), 43.5 (298.9), 27.9 (304.2), 18.4 (309.5), 14.5 (314.8), 10.9 (320.1), 8.91 (325.4), 6.35 (330.7), and 5.06 (335.9). The corresponding values for $[K(tmec12)]^+$ are 111 (288.3), 51.1 (293.6), 27.4 (298.9), 13.2 (304.2), 7.80 (309.5), 4.88 (314.8), 3.12 (320.1), 2.00 (325.4), 1.06 (330.7), and 0.74 (336.0). The data derived for $[Li(tmec12)]^+$ are similar to those derived from ^7Li NMR spectroscopy (Table 2). At 298.2 K, the rate of tmec12 exchange on $[K(tmec12)]^+$ is much slower than that of enantiomerization and is characterized by markedly different activation parameters consistent with the two processes operating independently of each other. (Intermolecular exchange in the $[Na(tmec12)]^+$ system remains in the slow exchange limit up to the boiling point of methanol-^{12}C-d_4.) As enantiomerization of $[Li(tmec12)]^+$ and the Na^+ and K^+ analogues occurs much more rapidly than intermolecular tmec12 exchange for all three complexes and metal ion exchange for the first two complexes, its mechanism may involve either a concerted twisting process in which all bonds remain intact, or a sequence of metal−oxygen bond breaking and making processes in which transient intermediates with monodentate pendant arms participate. No clear trend is apparent in the variations in kinetic data for either enantiomerization or tmec12 exchange consistent with changes in M^+ producing differing contributions through bonding interactions and ligand strain in $[M(tmec12)]^+$.

$$[M(tmec12)]^+ + *tmec12 \underset{k_d}{\overset{k_d}{\rightleftharpoons}} [M(*tmec12)]^+ + tmec12 \quad (3)$$

Acknowledgment. Funding of this study by the Australian Research Council and the University of Adelaide, and the award of an Australian Postgraduate Research Award to A.K.W.S. are gratefully acknowledged.

IC9509995

(21) Buøen, S.; Dale, J.; Groth, P.; Krane, J. *J. Chem. Soc., Chem. Commun.* **1982**, 1172−1174.